The Journal of the Acoustical Society of America

SEPTEMBER 07 2022

Leaky wave characterisation using spectral methods

Evripides Georgiades ; Michael J. S. Lowe ; Richard V. Craster

Check for updates

J. Acoust. Soc. Am. 152, 1487–1497 (2022)
https://doi.org/10.1121/10.0013897

View Online
Export Citation

05 July 2024 14:23:42



ASA
ACOUSTICAL SOCIETY OF AMERICA

JASA ARTICLE

Leaky wave characterisation using spectral methods

Evripides Georgiades,[a] Michael J. S. Lowe, and Richard V. Craster[b]
Department of Mechanical Engineering, Imperial College London, London SW7 1AY, United Kingdom

ABSTRACT:
Leaky waves are an important class of waves, particularly for guiding waves along structures embedded within another medium; a mismatch in wavespeeds often leads to leakage of energy from the waveguide, or interface, into the medium, which consequently attenuates the guided wave. The accurate and efficient identification of theoretical solutions for leaky waves is a key requirement for the choices of modes and frequencies required for non-destructive evaluation inspection techniques. We choose a typical situation to study: an elastic waveguide with a fluid on either side. Historically, leaky waves are identified via root-finding methods that have issues with conditioning, or numerical methods that struggle with the exponential growth of solutions at infinity. By building upon a spectral collocation method, we show how it can be adjusted to find exponentially growing solutions, i.e., leaky waves, leading to an accurate, fast, and efficient identification of their dispersion properties. The key concept required is a mapping, in the fluid region, that allows for exponential growth of the physical solution at infinity, whilst the mapped numerical setting decays. We illustrate this by studying leaky Lamb waves in an elastic waveguide immersed between two different fluids and verify this using the commercially available software DISPERSE.
© *2022 Author(s). All article content, except where otherwise noted, is licensed under a Creative Commons Attribution (CC BY) license (http://creativecommons.org/licenses/by/4.0/).* . https://doi.org/10.1121/10.0013897
(Received 5 April 2022; revised 22 July 2022; accepted 17 August 2022; published online 7 September 2022)
[Editor: James F. Lynch] Pages: 1487–1497

05 July 2024 14:23:42

I. INTRODUCTION

Ultrasonic guided waves are of enduring interest for non-destructive evaluation (NDE), where guided waves, such as Lamb waves,[1] are utilised for the inspection or structural health monitoring of single or multilayered systems of plates or pipes;[2–5] the complexities and characteristics of Lamb wave propagation for different systems and media are of paramount importance in identifying the appropriate choices in terms of frequencies and modes.[6] The route to effective inspection techniques depends critically upon predictive models focused on identifying the dispersion curves and associated stress and displacement fields, which have consequentially been the focus of much attention.

Leaky waves arise in immersed guiding structures: it is common for a structure of interest to consist of an elastic waveguide partially in contact with or fully immersed in fluids. In this scenario, the Lamb waves change their character as energy is no longer necessarily confined within the boundaries of a solid waveguide. When coupled to inviscid fluid(s) of infinite extent, two types of guided waves arise.[7] The first are guided waves remaining confined to the solid and immediately-adjacent fluid because their wavespeeds are below the speed of bulk waves in the adjacent fluid; these include, at high frequencies, Scholte waves.[8] These are not the focus of this article. The second type of guided wave has energy leakage, in the form of acoustic energy radiation from the waveguide into the adjacent fluid(s). This leads to attenuation, i.e., decay in amplitude, along the waveguide, and modes in the fluid(s) whose amplitudes grow exponentially in the direction transverse to the waveguide. These are known as leaky Lamb waves[9–11] and are the focus of this study.

A key role in multiple areas of wave physics is played by leaky waves, for instance, in guiding structures in electromagnetism,[12] where a mismatch of refractive indices between waveguide and exterior medium leads to energy leakage and analogous leaky waves. A comprehensive recent review,[13] in the electromagnetic waveguiding setting, usefully rationalises the phenomenon of the exponential growth of leaky waves and outlines applications in optics and electromagnetism. In acoustics and elasticity, leaky Rayleigh waves feature prominently in acoustic microscopy,[14] in material characterisation of the waveguide[15] or of the exterior fluid,[16] and underwater structural acoustics,[17] while leaky Lamb waves[9,18] feature in the NDE of composites; there is, therefore, naturally considerable interest in their accurate identification.

An (initially counter-intuitive) exponential growth of amplitude at infinity and corresponding complex-valued roots of dispersion relations characterise leaky waves, and this results in numerical issues when cleanly attempting to identify their dispersion characteristics, while doing so remains a challenge.[19] For those unfamiliar with leaky waves, the exponential growth of the mode might appear to be perplexing and to contradict energy conservation; a schematic showing the origin of this growth can be seen in Fig. 1. We choose an observation point, P, along a waveguide with attenuating waves propagating along the

[a]Electronic mail: evripides.georgiades18@imperial.ac.uk
[b]Also at: Department of Mathematics, Imperial College London, London SW7 1AY, United Kingdom.

 ©Author(s) 2022.

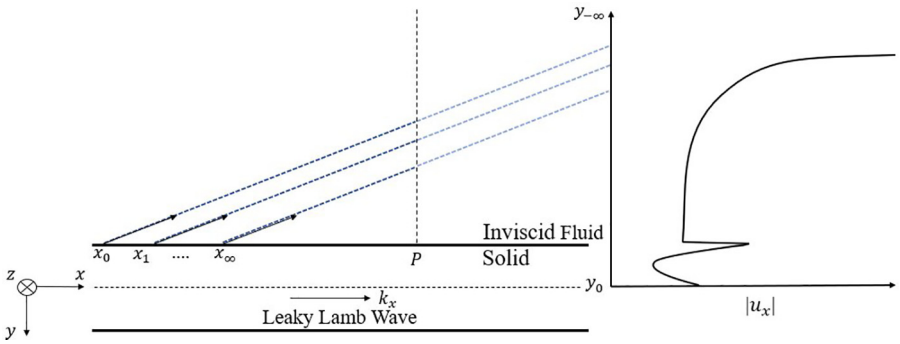


FIG. 1. (Color online) The exponential growth of leaky Lamb waves as a result of energy radiation at a fluid-solid interface.

waveguide with propagation constant k_x and then consider the far-field perpendicular to the guide. In the far-field, we are observing the result of energy that leaked from points preceding our observation point: the further we go back along the guide, the larger the amplitude of the energy that we observe. On this basis, the exponential growth we observe is actually a consequence of energy conservation.

For non-leaky guided waves, tools for the retrieval of dispersion characteristics are well-developed. Many numerical methods have been employed thus far, with one of the most established ones being partial wave root finding (PWRF). The general principle of PWRF routines is the production of a matrix formulation of the system in question, through a partial wave description of the problem, and the subsequent employment of root-finding routines for the evaluation of the roots of its characteristic equation and dispersion curves. There exist numerous such matrix formulations for single or multilayered systems, with the transfer matrix[20,21] and global matrix[22] methods being particularly appealing due to their relatively simple formulations. In fact, the commercially available software DISPERSE[23] utilises some of these PWRF techniques for the computation of dispersion characteristics of free and immersed systems, providing an excellent verification tool for the results of our study. An overview of the main matrix formulations used in PWRF routines for multilayered waveguides can be found in Lowe.[24]

Alas, PWRF routines have their limitations. To start with, their dependence on matrix formulations can result in spurious solutions when these matrices become computationally ill-conditioned. There are a couple of notable instances when this can happen. First, when the product of layer thickness with frequency is large and evanescent waves are to be found, some matrix formulations (e.g., transfer matrix) become unstable due to the existence of coefficients that grow and coefficients that decay within the matrices; this is known as the "large fd" problem.[25] Second, matrices can become computationally ill-conditioned when solutions near any of the bulk wavespeeds of a multilayered structure are being searched for. In that scenario, careful filtering needs to be applied to discard such solutions—a task that becomes increasingly difficult when genuine modes exist nearby. Another important caveat of PWRF is that the root-finding algorithm sometimes fails to capture a root of the characteristic equation and moves on to searching for the next one. A fine tuning of the convergence parameters of the algorithm fixes this problem but requires empirical knowledge of the existence of the mode that was missed. This is especially problematic when searching for the complex wavenumber solutions of leaky or attenuating modes. Complex roots are a step change in complexity beyond real roots and are an area in which root-finding routines are known to struggle.

An alternative to PWRF routines are the more recent methods based on a semi-analytical finite elements (SAFE) approach. An early popular work using SAFE was that of Gavric[26] on the study of waves propagating in a free rail. In that study, Hamilton's principle was applied for the derivation of the differential equations of motion, while finite elements (FEs) were used for the discretisation of the waveguide domain and the conversion of the equations of motion into a solvable eigenvalue problem. This allowed for the algebraic retrieval of all the roots of the characteristic equation in the form of eigensolutions. Moreover, SAFE allows for more flexibility when compared to the more traditional PWRF methods, as it can be used for spatially-irregular waveguides and complex structures where the latter becomes unstable. A few examples of this include the use of SAFE for the study of wave propagation in systems of viscoelastic media of arbitrary cross section,[27] in axisymmetric damped waveguides,[28] and in systems of waveguides coupled to infinite media.[29,30]

In line with the idea of discretising the domain of the structure in question and then obtaining a solution of the dispersion relation in the form of eigenvalues of an algebraic eigenvalue problem, spectral collocation methods (SCMs) have also been employed in recent years for the solution of guided wave problems.[31] The use of SCMs in physics,[32–34] can be very intuitive and numerically robust, making them an accessible tool for the algebraic solution of differential equations in the form of eigenvalue problems. Also, just like SAFE, and very importantly to our study of leaky waves, SCMs guarantee the retrieval of all solutions of the differential equation, including complex-valued ones. Most notably, the use of global interpolants, such as polynomials or trigonometric functions, as opposed to local ones, like the piecewise polynomials used in FE models, makes for an improved convergence rate of discretisation and accuracy of the solution when compared to SAFE methods.

Adamou and Craster[31] presented solutions for guided waves in simple cylindrical geometries, using SCMs with

05 July 2024 14:23:42

https://doi.org/10.1121/10.0013897

Chebyshev polynomials, demonstrating their potential applications in the field of guided waves. Following that, Karpfinger *et al.*[35] successfully used spectral collocation to study multilayered cylindrical structures consisting of isotropic media, Zharnikov *et al.*[36] used SCMs to study and plot the dispersion curves of an inhomogeneous anisotropic waveguide, and Quintanilla *et al.*[37–39] utilised the flexibility of SCMs for the study of flat and cylindrical multilayered viscoelastic and generally anisotropic systems.

The studies mentioned above focus on closed waveguide domains; however, the existence of open fluid domain(s) adjacent to the waveguide constitutes a much harder problem, with leaky waves posing a particularly difficult challenge due to the exponential growth of their amplitude far into the open domain(s). While attempting to solve for a fluid-loaded waveguide, root-finding techniques on the characteristic equation of Lamb waves[23,40,41] suffer from the aforementioned limitation of missing solutions of PWRF methods, while the often purely complex solutions to be found increase this occurrence. As a result, PWRF can be quite cumbersome when it comes to solving for leaky wave characteristics.

To overcome the issues of PWRF and complex roots, researchers have recently turned their attention to the discretisation of the domains of their problem to obtain algebraic solutions through eigenvalue problems. Mazotti *et al.*[42] presented a solution in which a SAFE discretisation of the closed waveguide domain was combined with a two-and-a-half-dimensional boundary element method to represent an unbounded fluid surrounding. To obtain a solution, contour integrals on areas of the complex plane where solutions may lie were performed. It was concluded that, in addition to the *a posteriori* knowledge of areas of the complex plane where possible solutions might exist, the formulation would be numerically unstable when the guided modes' poles lie close to the compressional wavespeed in the fluid. Another solution method was presented by Kiefer *et al.*,[19] where SCMs were implemented for the discretisation of the waveguide domain of a plate loaded on one or both sides by an inviscid fluid, the fluid being identical on both sides in the double-sided case. In that study, interface and boundary conditions were used to account for fluid loading, and a nonlinear eigenvalue problem, in terms of the wavenumber along the length of the waveguide, was produced. Through a change of variables,[43] the resulting nonlinear eigenvalue problem was reduced to a polynomial one and was later solved by a companion matrix linearisation[44] and the use of traditional eigenvalue problem solvers. This method can handle both leaky and trapped modes in a single-sided fluid-loaded plate; however, to the best of our knowledge, there is no suitable change of variables to reduce and solve the nonlinear eigenvalue problem that is presented by a waveguide in contact with two different inviscid fluids.

Alternatively, one could avoid having to deal with a nonlinear eigenvalue problem by effectively discretising the open fluid domain(s) and producing a linear problem. Unfortunately, the difficulties associated with accurately capturing the exponential growth of leaky waves in such a discretisation often force the derivation of elaborate discretisation techniques, such as the use of absorbing layers or absorbing boundary conditions. Fan *et al.*[45] implemented a SAFE method to model the propagation of leaky waves along an immersed waveguide with arbitrary non-circular cross section. A linear eigenvalue problem was achieved via the discretisation of the fluid domain through the application of an absorbing region. Quintanilla[46] utilised SCMs together with a perfectly matched layer (PML), while Treyssède *et al.*[7] deployed a SAFE discretisation together with a PML, to deal with the infinite surrounding medium. The accuracy of such models is, however, considerably dependent on the choice of absorbing layers, which in turn is dependent on the nature of the problem and its specific solutions. This means that these choices cannot be made for the general case in advance of performing the solution, a further complicating feature.

Here, we overcome the various difficulties outlined earlier, and we develop a SCM for the solution of leaky Lamb waves propagating along a waveguide that is in contact with two different inviscid fluid half-spaces. This new solution is applied and demonstrated using a specific example of a flat elastic plate with a different inviscid fluid half-space on each side. However, the solution has powerful generic potential that we believe will enable all classes of leaky waves to be solvable in follow-on developments.

For the discretisation of the closed waveguide domain, Chebyshev polynomials are used. It is worth noting that SAFE could have also been chosen here for the discretisation of the waveguide domain. We opt not to make that choice as the simple geometry of the elastic waveguide does not require the spatial versatility of SAFE, while, on the other hand, it allows for the favourable spectral accuracy of spectral collocation to be easily exploited. To deal with the open fluid half-spaces and the inherent exponential growth of leaky waves, a new technique for the discretisation of the open domains, which is based on rational Chebyshev polynomials and does not require the use of any absorbing boundaries, is presented here. A polynomial eigenvalue problem is then produced and solved using a companion matrix linearisation and conventional numerical solvers. Finally, the dispersion characteristics and displacement fields of leaky Lamb waves are computed. The case we present here is verified via DISPERSE, to demonstrate the ability of our method to produce accurate results. This is, however, without a loss of generality of our method.

This paper is organised as follows: Sec. II presents a brief summary of the theory relevant to the solution of the leaky Lamb wave problem of a waveguide in contact with two different inviscid fluid half-spaces. This is followed by a description of the discretisation method in Sec. III and a discussion of our results in Sec. IV.

II. THEORY

We consider a homogeneous, isotropic, linear-elastic waveguide of infinite extent in the x and z directions and

05 July 2024 14:23:42

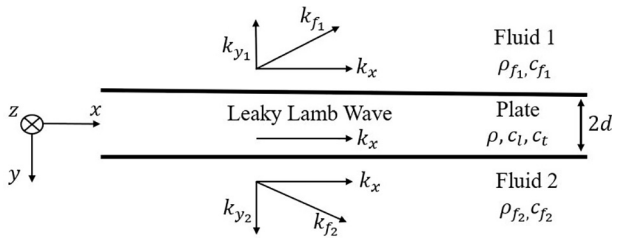


FIG. 2. Schematic of an elastic waveguide of thickness $2d$, infinite extent in the x and z directions, density ρ, longitudinal wavespeed c_l, and transverse wavespeed c_t, lying between two inviscid fluids of densities ρ_{f_1} and ρ_{f_2} and wavespeeds c_{f_1} and c_{f_2}, respectively.

finite thickness, $2d$, which is immersed between two inviscid fluids. The fluids can be different above and below the waveguide and have densities ρ_{f_1} and ρ_{f_2} and wavespeeds c_{f_1} and c_{f_2}, respectively, while the waveguide has density ρ, longitudinal wavespeed c_l, and transverse wavespeed c_t. A schematic of the cross section of the waveguide, also showing the coordinate axes, is shown in Fig. 2.

The centreline of the waveguide is along $y=0$, and the axis orientation has waves propagating in the positive x direction with wavenumber k_x. For given angular frequency, ω, the phase velocity is given by $c_{ph} = \omega/\Re(k_x)$, and attenuation in the propagation direction is $\alpha_x = \Im(k_x)$, with $\Re(\cdot)$ and $\Im(\cdot)$ denoting real and imaginary components of a complex number. Waves with displacements in the z direction decouple from those with displacements in the x and y directions;[47] the latter encompass the leaky Lamb waves that we aim to determine, and hence we only require displacements $\bar{u}_x$, $\bar{u}_{x_{f_1}}$, and $\bar{u}_{x_{f_2}}$ and $\bar{u}_y$, $\bar{u}_{y_{f_1}}$, and $\bar{u}_{y_{f_2}}$.

We denote with $\bar{\boldsymbol{u}} = (\bar{u}_x, \bar{u}_y, 0)^T$ the displacement vector in the waveguide and by $\bar{\boldsymbol{u}}_{f_1}$ and $\bar{\boldsymbol{u}}_{f_2}$ the displacement vectors in the two fluids. By employing a Helmholtz decomposition,[48,49] they can be written as

$$\bar{\boldsymbol{u}}_{f_1} = \begin{pmatrix} \bar{u}_{x_{f_1}} \\ \bar{u}_{y_{f_1}} \\ 0 \end{pmatrix} = \nabla \bar{\phi}_{f_1}, \quad \bar{\boldsymbol{u}}_{f_2} = \begin{pmatrix} \bar{u}_{x_{f_2}} \\ \bar{u}_{y_{f_2}} \\ 0 \end{pmatrix} = \nabla \bar{\phi}_{f_2}, \tag{1}$$

with $\bar{\phi}_{f_1}$ and $\bar{\phi}_{f_2}$ the displacement potentials in the two fluids. The quantities $\bar{u}_x$, $\bar{u}_y$, $\bar{\phi}_{f_1}$, and $\bar{\phi}_{f_2}$ are functions of x, y, and t. We are assuming plane harmonic waves in the form

$$\bar{u}_x(x,y,t) = u_x(y)\exp\left(i(k_x x - \omega t)\right), \tag{2}$$

with the common exponential factor henceforth omitted and considered understood, and similarly for $\bar{u}_y(x,y,t)$, $\bar{\phi}_{f_1}(x,y,t), \bar{\phi}_{f_2}(x,y,t)$.

The two-dimensional wave motion in the isotropic solid is governed by the momentum equations[50]

$$\rho\omega^2 u_x - (\lambda+2\mu)k_x^2 u_x + (\lambda+\mu)ik_x\frac{\partial u_y}{\partial y} + \mu\frac{\partial^2 u_x}{\partial y^2} = 0, \tag{3}$$

$$\rho\omega^2 u_y - \mu k_x^2 u_y + (\lambda+\mu)ik_x\frac{\partial u_x}{\partial y} + (\lambda+2\mu)\frac{\partial^2 u_y}{\partial y^2} = 0, \tag{4}$$

with λ and μ the elastic Lamé parameters. We follow Nayfeh and Nagy[18] for the fluids, specialising their viscous model to be inviscid, to obtain the fluid momentum equation[50]

$$\rho_{f_j}\omega^2\phi_{f_j} - \lambda_{f_j}k_x^2\phi_{f_j} + \lambda_{f_j}\frac{\partial^2\phi_{f_j}}{\partial y^2} = 0, \tag{5}$$

with the subscripts $j=1,2$ corresponding to the fluids above and below the waveguide, respectively, and $\lambda_{f_j} = \rho_{f_j}c_{f_j}^2$ in each fluid.

To fully describe wave motion in the immersed waveguide system, in addition to Eqs. (3)–(5), interface conditions are required. For a two-sided fluid-loaded system, these are the continuity of normal stress and normal displacement, and the vanishing of shear stress at the two interfaces.[49] They are explicitly expressed[50] as

$$\left[(\lambda+2\mu)\frac{\partial u_y}{\partial y} + \lambda ik_x u_x + \rho_{f_j}\omega^2\phi_{f_j}\right]\Big|_{y=\pm d} = 0, \tag{6}$$

$$\left[ik_x u_y + \frac{\partial u_x}{\partial y}\right]\Big|_{y=\pm d} = 0, \tag{7}$$

$$\left[\frac{\partial\phi_{f_j}}{\partial y} - u_y\right]\Big|_{y=\pm d} = 0. \tag{8}$$

Wave propagation in the waveguide is captured by a single wavenumber, k_x, whereas the inhomogeneous bulk waves that propagate in the fluids, at an angle from the waveguide (see Fig. 2), require additional wavenumbers; these represent partial waves propagating in the transverse y direction. The aforementioned wavenumbers are denoted by k_{y_1} and k_{y_2} for the two fluids. Similar to k_x, the real parts of these transverse wavenumbers describe the speed of propagation of the waves in the y direction, and their imaginary parts describe their attenuation or growth as they propagate along the same direction. We define the propagation wave vectors of these inhomogeneous bulk waves as

$$\mathbf{k}_{f_1} := \begin{pmatrix} k_x \\ k_{y_1} \end{pmatrix} \quad \text{and} \quad \mathbf{k}_{f_2} := \begin{pmatrix} k_x \\ k_{y_2} \end{pmatrix}. \tag{9}$$

For inviscid fluids, the magnitude of these wave vectors is real and is given by

$$k_{f_j} := |\mathbf{k}_{f_j}| = \frac{\omega}{c_{f_j}}, \quad \text{for} \quad j=1,2, \tag{10}$$

and the following trigonometric relations hold:

$$k_{f_j}^2 = k_x^2 + k_{y_j}^2 \quad \text{for } j=1,2. \tag{11}$$

Consequently, the longitudinal wave potentials, ϕ_{f_1} and ϕ_{f_2}, in the two fluid half-spaces are[18,51]

$$\phi_{f_1}(y) = A_1\exp\left(-ik_{y_1}(y+d)\right), \tag{12}$$

$$\phi_{f_2}(y) = A_2\exp\left(ik_{y_2}(y-d)\right), \tag{13}$$

where A_1 and A_2 are constants.

05 July 2024 14:23:42

https://doi.org/10.1121/10.0013897

One approach to formulating the problem mathematically is to substitute Eqs. (12) and (13) in Eqs. (5)–(8), discretise the waveguide, and arrive at a nonlinear eigenvalue problem,[19] where the nonlinearity of the problem is a result of the square root term arising from the use of Eqs. (10) and (11). For a single fluid, either on one side or on both sides, and leaky Lamb waves in a waveguide, Kiefer *et al.*[19] employ a spectral collocation method using Chebyshev polynomials to discretise the waveguide; a neat change of variables[43] reduces the algebraic nonlinear eigenvalue problem to a polynomial eigenvalue problem, which is then solvable with well-established methods. We are aiming at a general approach for leaky waves in immersed waveguides or pipes, while fluid coupling of even straight waveguides, by two different fluids, leads to a more complicated nonlinear eigenvalue problem that appears not to reduce quite so pleasantly. We employ a spectral collocation discretisation of both the waveguide and of the two open spaces of the inviscid fluids, the key being the discretisation of the fluids, which we describe in detail in Sec. III. This discretisation results in a polynomial eigenvalue problem with the complex wavenumber k_x as its eigenvalue and the wave displacements, complemented by the wave amplitudes of Eqs. (12) and (13), as the eigenvector; this deals with the exponential growth of the leaky modes without the need to use any absorbing layers or PMLs in the fluid domains and leads to an eigenvalue problem that can be solved with standard methods.

III. DISCRETISATION

The discretisation of both the waveguide and the open fluid domains is done using spectral collocation.[33,52] It is worth noting that the discretisation method to be presented in this section is not unique to spectral collocation. However, for the problem of planar geometry discussed in this article, spectral collocation was advantageous to implement.

In brief, spectral collocation revolves around creating differentiation matrices: consider a continuous function $g(y)$, with y in some domain $\mathcal{C}$, whose derivative is to be approximated. A set of distinct interpolation points $\{p_i\}_{i=1}^{N} \in \mathcal{C}$, for some $N \in \mathbb{N}$, also known as collocation points,[34,52] are fixed, and then $\boldsymbol{g}$, the vector of g evaluated at the collocation points, and $\boldsymbol{g}^{(l)}$, the vector of their lth derivatives, are related via the lth differentiation matrix of g, $D^{(l)}$, such that

$$\boldsymbol{g}^{(l)} \approx D^{(l)}\boldsymbol{g}. \tag{14}$$

The identification of the collocation points is the key step, and a common choice, when $\mathcal{C}$ is a bounded interval and g is a smooth function, is that of Chebyshev collocation points, for which the Chebyshev differentiation matrices exhibit spectral accuracy.[34,52] This accuracy, together with their flexibility and established use in guided wave problems,[19,31,37] motivates our use of them for the waveguide region. To treat the open spaces of fluid, we use a generalisation of Chebyshev methods—specifically of rational Chebyshev[34] approaches; these have been used for guided waves in optics, i.e., in the modal analysis of a multilayered optical waveguide.[53] Rational Chebyshev nodes arise from the mapping of Chebyshev collocation nodes onto an open space, infinite or semi-infinite, and preserve the performance benefits of traditional Chebyshev differentiation matrices. We use the differentiation matrix suite provided by Weideman and Reddy[32] to obtain the first and second order differentiation matrices, denoted by $D^{(1)}$ and $D^{(2)}$, respectively, using N Gauss–Lobatto Chebyshev collocation points

$$s_i = -\cos\left(\frac{(i-1)\pi}{N-1}\right), \tag{15}$$

for $i = 1, \ldots, N$ and $s_i \in [-1, 1]$.

The treatment of the waveguide follows:[31] taking N_p as the number of collocation points in the waveguide, multiplication by d maps the N_p collocation points of Eq. (15) onto the bounded interval of the waveguide, $[-d, d]$; these points as contained in the vector $\boldsymbol{y}_p = \{y_p^i = ds_i\}_{i=1,\ldots,N_p}$. The corresponding differentiation matrices, approximating the first and second order derivatives in the solid domain, are $D_p^{(1)} = (1/d)D^{(1)}$ and $D_p^{(2)} = (1/d^2)D^{(2)}$.

To treat the fluid domains and build in the exponential growth of leaky waves, we follow a different approach. Consider the complex variable mappings $h_{f_1} : [-1, 1] \to \mathbb{C}$ and $h_{f_2} : [-1, 1] \to \mathbb{C}$ given by

$$h_{f_1} : s \to y = -d - \zeta_{f_1}\frac{1-s}{1+s}, \tag{16}$$

$$h_{f_2} : s \to y = d + \zeta_{f_2}\frac{1+s}{1-s}, \tag{17}$$

with $\zeta_{f_1}, \zeta_{f_2} \in \mathbb{C}$; the choice of the two complex parameters ζ_{f_1} and ζ_{f_2} plays an important role in our discretisation of the fluid domains as importantly we are mapping a real interval to a semi-infinite interval in complex space. To guide their choice, we note that the wave potentials in Eqs. (12) and (13) require the transverse wavenumbers k_{y_1} and k_{y_2} to lie in the fourth complex quadrant (positive real and negative imaginary parts) to represent outgoing and exponentially growing leaky waves.

The key step is the mapping to complex space, and not to a real domain: a choice of positive real numbers ζ_{f_1} and ζ_{f_2}, such as the one made in previous work on optical waveguides,[53] maps the collocation points of Eq. (15), through h_{f_1} and h_{f_2}, to $[-\infty, -d]$ and $[d, \infty]$, respectively. The implicit exponential growth of leaky waves prevents the QZ-algorithm of conventional eigenvalue solvers from reliably retrieving the solution and requires the use of perfectly matched, absorbing layers or outgoing wave boundary conditions at infinity, which simply transfers the numerical problems normally encountered to elsewhere in the problem. We note that, within such PMLs, a map to complex space, to appropriately adjust the leaky PML solutions to decay,[7] allows leaky wave solutions.

We take $\zeta_{f_1}, \zeta_{f_2} \in \mathbb{C}$, i.e., complex, and to lie in the first complex quadrant (positive real and imaginary parts).

05 July 2024 14:23:42

This choice has h_{f_1} mapping the collocation points of Eq. (15) to a path in the third complex quadrant (negative real and imaginary parts), with the point at 1 being mapped to the interface at $y=-d$. Similarly, h_{f_2} maps the collocation points to a path in the first complex quadrant, with the point at –1 being mapped to the interface at $y=d$. These result in a discretisation of two paths in the complex quadrants, which we denote by $\mathbb{C}_{f_1}$ and $\mathbb{C}_{f_2}$, respectively.

The analytic continuations of each of the fluid wave potentials of Eqs. (12) and (13), with domains of definition the complex paths $\mathbb{C}_{f_j}$, are henceforth referred to as the complex fluid wave potentials and are denoted by $\tilde{\phi}_{f_j}$. Both of $\tilde{\phi}_{f_1}$ and $\tilde{\phi}_{f_2}$ still satisfy the momentum equations of Eq. (5) for the two fluids and all six of the interface conditions of Eqs. (6)–(8). Importantly, choices of ζ_{f_1}, ζ_{f_2} make the numerical problem have exponential decay, even for leaky modes, while simultaneously attaining the physical solution on the two fluid-solid interfaces, as the choice of mapping guarantees a collocation point on the real space of those interfaces; the inhomogeneous plane waves in the two fluids mean that values at the interfaces fully determine motion in each fluid; hence, solving the complex-valued problem arising from using h_{f_1} and h_{f_2} gives the physical solution for the leaky waves.

Using the mappings, we can create differentiation matrices. Taking N_{f_1} and N_{f_2} as the number of collocation points for each of the fluids, we set the vector $\boldsymbol{y}_{f_1} = \{y_{f_1}^m = h_{f_1}(s_m)\}_{m=1,\ldots,N_{f_1}}$ of the collocation points in $\mathbb{C}_{f_1}$ and the vector $\boldsymbol{y}_{f_2} = \{y_{f_2}^n = h_{f_2}(s_n)\}_{n=1,\ldots,N_{f_2}}$ of the collocation points in $\mathbb{C}_{f_2}$; repeated use of the chain rule gives the differentiation matrices for the fluids in the two complex domains. The $N_{f_1}\times N_{f_1}$ differentiation matrices for the fluid at the top of the plate are given by

$$D_{f_1}^{(1)} = \mathrm{diag}\left(\frac{2\zeta_{f_1}}{\left[\zeta_{f_1} - (\boldsymbol{y}_{f_1} + \boldsymbol{d})\right]^2}\right) D^{(1)}, \tag{18}$$

$$D_{f_1}^{(2)} = \mathrm{diag}\left(\frac{4\zeta_{f_1}}{\left[\zeta_{f_1} - (\boldsymbol{y}_{f_1} + \boldsymbol{d})\right]^3}\right) D^{(1)} + \mathrm{diag}\left(\frac{4\zeta_{f_1}^2}{\left[\zeta_{f_1} - (\boldsymbol{y}_{f_1} + \boldsymbol{d})\right]^4}\right) D^{(2)}, \tag{19}$$

and the $N_{f_2}\times N_{f_2}$ ones for the fluid at the bottom of the plate are given by

$$D_{f_2}^{(1)} = \mathrm{diag}\left(\frac{2\zeta_{f_2}}{\left[\zeta_{f_2} + (\boldsymbol{y}_{f_2} - \boldsymbol{d})\right]^2}\right) D^{(1)}, \tag{20}$$

$$D_{f_2}^{(2)} = \mathrm{diag}\left(\frac{-4\zeta_{f_2}}{\left[\zeta_{f_2} + (\boldsymbol{y}_{f_2} - \boldsymbol{d})\right]^3}\right) D^{(1)} + \mathrm{diag}\left(\frac{4\zeta_{f_2}^2}{\left[\zeta_{f_2} + (\boldsymbol{y}_{f_2} - \boldsymbol{d})\right]^4}\right) D^{(2)}. \tag{21}$$

Here, $\boldsymbol{d} = (d, \ldots, d)^T$ is a column vector of appropriate size, and likewise for $\boldsymbol{\zeta}_{f_1}$ and $\boldsymbol{\zeta}_{f_2}$. The diagonal matrices in Eqs. (18)–(21) are the matrices whose diagonals are the expressions in parenthesis, evaluated at each of the collocation points, and have zeros everywhere else.

Due to our choice of discretisation, now numerically extracting a decaying function rather than an exponentially growing one, the choice of boundary condition at infinity is relevant only insofar as we want to ensure the solution tends to zero at infinity; this is achieved by taking Dirichlet zero boundary conditions at the farthest collocation point in the complex space. This is applied by deleting the corresponding rows and columns of our differentiation matrices, as well as the corresponding collocation point. For the top fluid, we delete $y_{f_1}^1$ and the first rows and columns of $D_{f_1}^{(1)}$ and $D_{f_1}^{(2)}$, and for the bottom fluid, we delete $y_{f_2}^{N_{f_2}}$ and the last rows and columns of $D_{f_2}^{(1)}$ and $D_{f_2}^{(2)}$. The x and y displacements in the waveguide, each evaluated at the N_p collocation points within the domain of the solid, are given in vector form by $\mathbf{u}_x = [u_x(y_p^i)]_{i=1,\ldots,N_p}^T$ and $\mathbf{u}_y = [u_y(y_p^i)]_{i=1,\ldots,N_p}^T$, while the complex fluid wave potentials evaluated at the collocation points of each of the fluids are given by $\tilde{\boldsymbol{\Phi}}_{f_1} = [\tilde{\boldsymbol{\Phi}}_{f_1}(y_{f_1}^i)]_{i=2,\ldots,N_{f_1}}^T$ and $\tilde{\boldsymbol{\Phi}}_{f_2} = [\tilde{\boldsymbol{\Phi}}_{f_2}(y_{f_2}^i)]_{i=1,\ldots,N_{f_2}-1}^T$.

We can now proceed to generate the eigenvalue problem we wish to solve. We start by representing the differential operators of Eqs. (3)–(5), using the differentiation matrices $D_p^{(l)}$ and $D_{f_j}^{(l)}$, for $j=1,2$ and $l=1,2$, as the matrix operators

$$L_p = k_x^2 L_{p_2} + k_x L_{p_1} + L_{p_0}, \tag{22}$$

$$L_{f_j} = k_x^2(-\lambda_{f_j} I) + \rho_{f_j}\omega^2 I + \lambda_{f_j} D_{f_j}^{(2)}, \tag{23}$$

with L_{p_j} given by

$$L_{p_2} = \begin{bmatrix} -(\lambda+2\mu)I & 0 \\ 0 & -\mu I \end{bmatrix}, \tag{24}$$

$$L_{p_1} = \begin{bmatrix} 0 & i(\lambda+\mu)D_p^{(1)} \\ i(\lambda+\mu)D_p^{(1)} & 0 \end{bmatrix}, \tag{25}$$

$$L_{p_0} = \begin{bmatrix} \rho\omega^2 I + \mu D_p^{(2)} & 0 \\ 0 & \rho\omega^2 I + (\lambda+2\mu)D_p^{(2)} \end{bmatrix}. \tag{26}$$

In Eqs. (23)–(26), I is the identity matrix of appropriate size; these matrix operators allow us to write the equations of motion of the immersed plate problem as the eigenvalue problem

$$\tilde{L}\boldsymbol{u} = \mathbf{0}, \tag{27}$$

with

$$\tilde{L} = \begin{pmatrix} L_{f_1} & 0 & 0 \\ 0 & L_p & 0 \\ 0 & 0 & L_{f_2} \end{pmatrix}$$

05 July 2024 14:23:42

https://doi.org/10.1121/10.0013897

and $\mathbf{u} = [\tilde{\boldsymbol{\phi}}_{f_1}, \mathbf{u}_x, \mathbf{u}_y, \tilde{\boldsymbol{\phi}}_{f_2}]^T$. In Eqs. (22)–(26), we separate the matrix operators into k_x^2-dependent, k_x-dependent, and constant components; this is convenient for the polynomial eigenvalue problem formulation we use later. Similarly, we separate $\tilde{L}$, with $\tilde{L}_2$, $\tilde{L}_1$, and $\tilde{L}_0$ being the matrices for the k_x^2-dependent, k_x-dependent, and constant components, respectively: Eq. (27) is rewritten as

$$\left(k_x^2\tilde{L}_2 + k_x\tilde{L}_1 + \tilde{L}_0\right)\boldsymbol{u} = 0. \tag{28}$$

The final step is to incorporate the interface conditions Eqs. (6)–(8). To achieve this, we first write each of those interface conditions as rows of two $3 \times (N_{f_1} + 2N_p + N_{f_2} - 2)$ matrices. For simplicity, we represent those with two 3×4 matrices. Their first and last columns correspond to $\tilde{\boldsymbol{\phi}}_{f_1}$ and $\tilde{\boldsymbol{\phi}}_{f_2}$, whereas the second and third columns correspond to $\mathbf{u_x}$ and $\mathbf{u_y}$. The matrix of interface conditions at the top interface is

$$IC_{-d} = k_x \begin{bmatrix} 0 & i\lambda I & 0 & 0 \\ 0 & 0 & iI & 0 \\ 0 & 0 & 0 & 0 \end{bmatrix}\Bigg|_{y=-d} + \begin{bmatrix} \rho_{f_1}\omega^2 I & 0 & (\lambda+2\mu)D_p^{(1)} & 0 \\ 0 & D_p^{(1)} & 0 & 0 \\ D_{f_1}^{(1)} & 0 & -I & 0 \end{bmatrix}\Bigg|_{y=-d}, \tag{29}$$

where the elements are row vectors, representing the discrete evaluation of the differential operators of the interface conditions at the interface $y = -d$. This evaluation at $y = -d$ equates to picking the rows of the differential operators appearing in Eq. (29) that correspond to the collocation point at that interface. By our choice of discretisation, for the complex fluid potential of the fluid at the top of the plate, we need to pick the $(N_{f_1} - 1)$th row of the matrices, whereas for the plate displacements, we need to pick the first rows of the matrices.

Similarly, the matrix of interface conditions at the bottom interface is

$$IC_{d} = k_x \begin{bmatrix} 0 & i\lambda I & 0 & 0 \\ 0 & 0 & iI & 0 \\ 0 & 0 & 0 & 0 \end{bmatrix}\Bigg|_{y=d} + \begin{bmatrix} 0 & 0 & (\lambda+2\mu)D_p^{(1)} & \rho_{f_2}\omega^2 I \\ 0 & D_p^{(1)} & 0 & 0 \\ 0 & 0 & -I & D_{f_2}^{(1)} \end{bmatrix}\Bigg|_{y=d}. \tag{30}$$

The same convention for the evaluation of the differential operators is used here. For the evaluation at the interface $y = d$, we need to pick the first row of the operators for the complex fluid potential of the fluid at the bottom of the plate and the N_pth row of the operators for the plate displacements.

Second, we incorporate those interface conditions in $\tilde{L}$ by replacing the rows of $\tilde{L}$ that correspond to the two interfaces with rows from the interface conditions, as those were described in Eqs. (29) and (30). Again, due to our discretisation and construction of $\tilde{L}$ from the matrix differential operators of Eqs. (22) and (23), the rows of $\tilde{L}$ corresponding to the interface $y = -d$ are $N_{f_1} - 1$, N_{f_1}, and $N_{f_1} + N_p$. We replace each of those with a row from Eq. (29). Similarly, the rows of $\tilde{L}$ corresponding to the interface at $y = d$ are $N_{f_1} + N_p - 1$, $N_{f_1} + 2N_p - 1$, and $N_{f_1} + 2N_p$, and we replace each of those with a row from Eq. (30). Finally, we arrive at a matrix, L, with an analogous decomposition to the one of Eq. (28). The resulting polynomial eigenvalue problem is

$$\left(k_x^2 L_2 + k_x L_1 + L_0\right)\boldsymbol{u} = \mathbf{0}, \tag{31}$$

where for a given ω, k_x is our eigenvalue, and $\boldsymbol{u}$ is our eigenvector. To solve the polynomial eigenvalue problem, we employ a companion matrix linearisation[44] by setting $\boldsymbol{U} = [k_x\boldsymbol{u}, \boldsymbol{u}]^T$ and define the square companion matrices

$$A = \begin{bmatrix} -L_1 & -L_0 \\ I & 0 \end{bmatrix} \quad \text{and} \quad B = \begin{bmatrix} L_2 & 0 \\ 0 & I \end{bmatrix}, \tag{32}$$

with I the identity matrix of dimension $(N_{f_1} + 2N_p + N_{f_2} - 2) \times (N_{f_1} + 2N_p + N_{f_2} - 2)$. Then the eigenvalue problem of Eq. (31) is equivalent to the generalised linear eigenvalue problem,

$$(A - k_x B)\boldsymbol{U} = \mathbf{0}, \tag{33}$$

which is solvable with conventional generalised eigenvalue problem solvers, with eigenvalue k_x and eigenvector $\boldsymbol{U}$.

To summarise, using a spectral collocation discretisation, we were able to formulate and solve a polynomial eigenvalue problem that preserves the characteristics of leaky wave propagation in a waveguide immersed between two fluids of different wavespeeds. The key idea of our method was to model wave propagation in carefully selected paths in the complex plane rather than the physical fluid domains. This allowed us to search for exponentially decaying numerical solutions that fully and accurately describe the exponentially growing physical ones, without the need of solving non-linear eigenvalue problems or the use of PMLs or absorbing boundaries at infinity. Additionally, a very significant property of the new method is that it does not itself introduce attenuation to the material, in which respect it differs from PML. Thus, our method delivers correct solutions for the wave fields in the exterior domain without attenuating them. Importantly, this technique is not unique to SCMs, and the key principle can be utilised to accurately obtain solutions to problems where energy leakage in infinite media is observed.

IV. RESULTS AND DISCUSSION

The leaky wave SCM is now employed to find the dispersion curves of the leaky modes for an elastic waveguide

05 July 2024 14:23:42

with different inviscid fluids above and below the waveguide; these curves are validated with the commercially available software DISPERSE[23] as are the displacements obtained as the eigenvectors of the leaky SCM. DISPERSE is a well-established software designed for the generation of dispersion curves in multilayered media, embedded or *in vacuo*, using matrix techniques and a PWRF algorithm,[23,54] and it provides a good basis for comparison with our method as its reliability has been demonstrated in multiple scenarios.[55–59]

We choose a typical example and compute the dispersion curves of a 1 mm thick brass plate ($\rho = 8.4$ g/cm^3, $c_t = 2.2$ m/ms, $c_l = 4.4$ m/ms) loaded on the top side by water ($\rho_{f_1} = 1$ g/cm^3, $c_{f_1} = 1.5$ m/ms) and at the bottom side by diesel oil ($\rho_{f_2} = 0.8$ g/cm^3, $c_{f_2} = 1.25$ m/ms). For the choice of complex parameters ζ_{f_j}, consider the following discussion. For a complex wavenumber solution k_x and corresponding transverse wavenumbers k_{y_j}, Eqs. (12) and (13), with $y \in C_{f_j}$, describe the wave fields in the complex domains C_{f_j}. Those can equivalently be rewritten as

$$\tilde{\phi}_{f_1}(y) = A_1 \exp\left(-i\zeta_{f_1} k_{y_1} y\right) \quad \text{with } y \in [-\infty, 0], \tag{34}$$

$$\tilde{\phi}_{f_2}(y) = A_2 \exp\left(i\zeta_{f_2} k_{y_2} y\right) \quad \text{with } y \in [0, \infty]. \tag{35}$$

A convergence study[50] of Eqs. (34) and (35) reveals that a choice of ζ_{f_j}, such that

$$\Re(k_{y_j})\Im(\zeta_{f_j}) + \Re(\zeta_{f_j})\Im(k_{y_j}) > 0, \tag{36}$$

results in exponentially decaying potentials on the complex paths $\mathbb{C}_{f_j}$. For the leaky modes [$\Re(k_{y_j}) > 0$ and $\Im(k_{y_j}) < 0$] of concern in this study, Eq. (36) takes the form

$$\Im(\zeta_{f_j}) > -\Re(\zeta_{f_j}) \frac{\Im(k_{y_j})}{\Re(k_{y_j})}. \tag{37}$$

Without loss of generality, we make the choice of $\Re(\zeta_{f_j}) = 1$, maintaining in this way the span of the Gauss–Lobatto Chebyshev collocation points of Eq. (15), along the complex paths $\mathbb{C}_{f_j}$; we can without loss of generality choose $\Im(\zeta_{f_j}) > -\Im(k_{y_j})/\Re(k_{y_j})$.

The choice can be automated, and we use the following rule-of-thumb: we first solve for the same waveguide immersed in two identical inviscid fluids.[19] This is done twice, solving for a brass waveguide fully immersed in water and then in oil, each time recording the maximum value of the ratio $-\Im(k_y)/\Re(k_y)$ for leaky wave solutions in the frequency range of interest of our problem. These maximum ratios provide initial guesses for the ratios $-\Im(k_{y_j})/\Re(k_{y_j})$; in the angular frequency range 0–20 MHz, those were found to be less than 1.

In light of this, for the computation of dispersion curves with our SCM, we take the conservative choice of $\zeta_{f_j} = 1 + 10i$, satisfying in this way Eq. (37). As this translates to a rapidly decaying solution, we also choose a sufficient number of collocation points to capture this decay. A conservative choice is $N_p = N_{f_1} = N_{f_2} = 30$, which yields a convergent solution. We have investigated the stability of the algorithm regarding the choices of ζ_{f_j} and the numbers of collocation points, and the scheme is very robust, in the frequency range studied, to the choices taken. Despite that fact, we recognise that a more thorough investigation of these combinations is required to confidently and accurately obtain the full set of leaky wave solutions for all frequencies and every possible combination of solids and external fluids. The computation at 200 frequency points took a total of 40.36 s on a personal computer with a 32 GB RAM memory and an i7-10700 central processing unit (CPU).

The SCM results are compared with those from DISPERSE in Fig. 3 with pleasing agreement for both the phase velocity and attenuation. There are infinitely many possible modes that can propagate through the waveguide, and we have performed filtering prior to plotting, so we illustrate those modes of most physical interest. The filtering comprises a positively propagating wave requirement with $\Re(k_x) > 0$ and attenuation with $\Im(k_x) > 0$ and $|k_x| \neq \infty$. We would also like to direct the reader's attention to the fact that only leaky modes are depicted in Fig. 3, which are the traditionally more complex solutions to obtain due to the exponential growth of amplitude in both half-spaces of fluids. The full

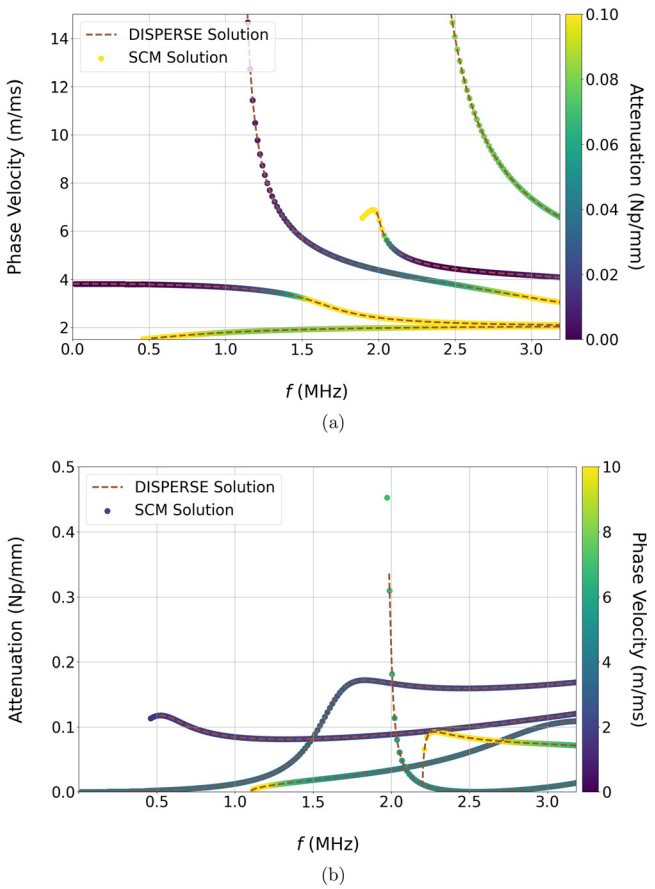


FIG. 3. (Color online) Comparison of dispersion curves obtained from our SCM and from DISPERSE, for a 1 mm thick brass plate, loaded on one side by water and on the other by diesel oil. (a) plots phase velocity against frequency, while (b) plots attenuation against frequency.

05 July 2024 14:23:42

https://doi.org/10.1121/10.0013897

set of solutions, that is, modes that only leak in one of the fluids or trapped modes, can also be attained with an appropriate choice of complex parameters ζ_{fj}. For plotting purposes, we made an arbitrary choice of cut-off attenuation at 1 Np/mm.

The SCM conveniently retrieves the values of the amplitudes of the fluid potential and the displacements in the solid from the eigenvector through $\boldsymbol{U}$; as these fully describe the acoustic fields in the fluids and the solid, we get the whole of the wave field without any extra effort. The displacements in the fluids are computed using the Helmholtz decomposition of the fluid displacements in Eq. (1) and the wave potentials in Eqs. (12) and (13). Using the water-brass-oil system of Fig. 3, we compare the y-dependent component of the displacements, in both the direction of propagation and the normal direction, with the corresponding DISPERSE solution. In Fig. 4, we compare the displacements of an arbitrarily selected frequency-phase velocity pair $(f, c_{ph}) \approx (2.02, 6.18)$, taken from Fig. 3, again showing a good match. The SCM solutions are obtained as an eigenvector of a polynomial eigenvalue problem, and any scalar multiple remains a solution. To fix upon a solution, we impose u_x at the interface $y = -d$ to be the same for both SCM and DISPERSE solutions.

V. CONCLUSION

The leaky Lamb wave problem, for a plate loaded on both sides by two different fluids, is an exemplar of leaky waves and exhibits the key difficulty of studying such systems; the nonlinear eigenvalue problem is difficult to solve, a neat change of variables to transform it is not easily available, and the exponential growth poses a numerical challenge to the retrieval of accurate solutions. To overcome this inherent difficulty, a mapping of the fluid domains onto paths in complex domains was performed; the exponential growth is then built into this, and we can reformulate as a polynomial eigenvalue problem solved using standard solvers; thence, we obtain the complete physical solution robustly, accurately, and without the need of user

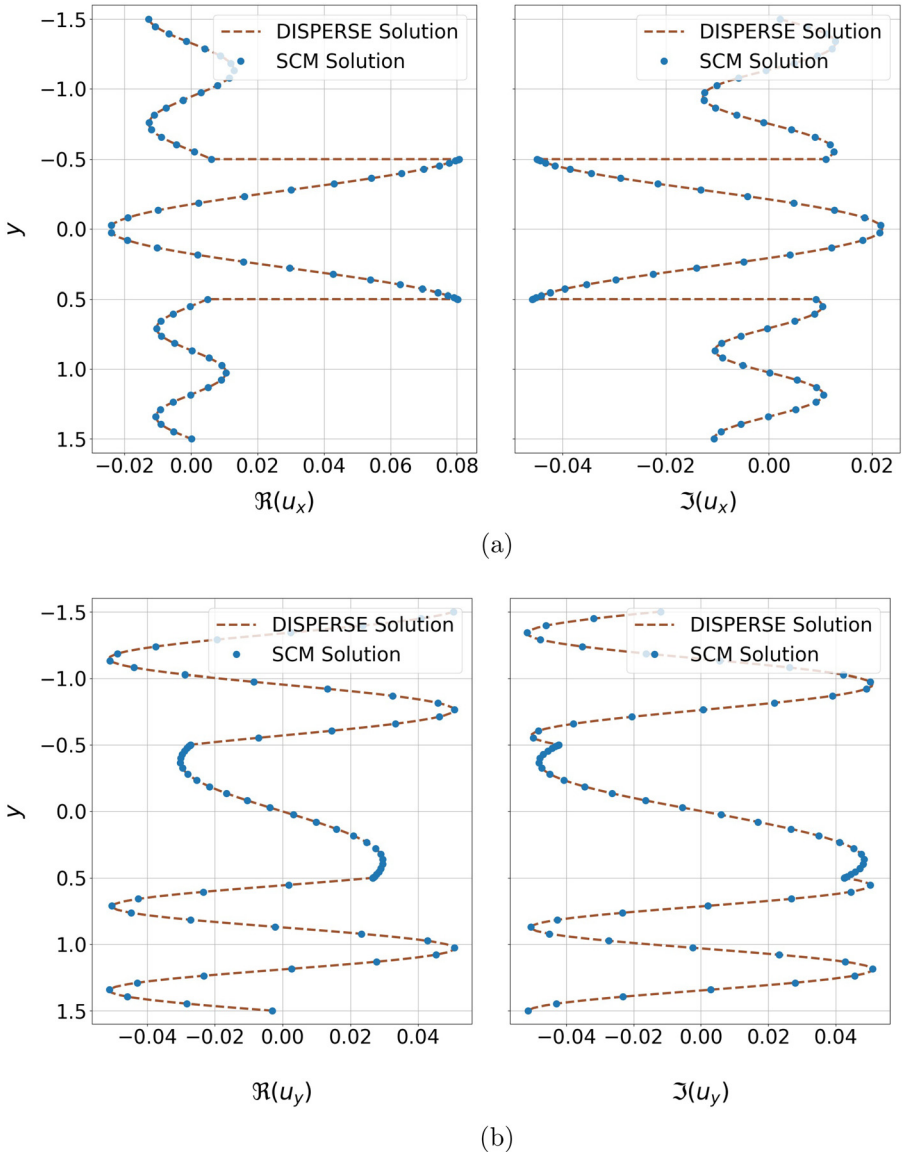


FIG. 4. (Color online) Mode shapes displaying the y-dependent component of displacements for a 1 mm thick brass plate loaded on one side by water and on the other by diesel oil, for the frequency-phase velocity pair $(f, c_{ph}) \approx (2.02, 6.18)$. (a) plots the real and imaginary parts of $u_x(y)$, and (b) plots the real and imaginary parts of $u_y(y)$. In both plots, the results from DISPERSE and the scaled results from our SCM are presented.

05 July 2024 14:23:42

intervention—each of which attributes, or a combination of them, is a potential challenge to other existing methods. The SCM, based on Chebyshev approaches to discretise both the open and closed domains of our system, provides our method with speed, accuracy, and robustness whilst keeping the eigenvalue systems compact. The formulation leads to systems amenable to standard eigensolvers, and we are able to obtain all the complex wavenumbers and displacement fields of leaky Lamb waves for any given frequency.

The complex mapping and the treatment of the exponential growth of the leaky waves of our system are not unique to the planar elastic waveguiding problem: the methodology we have introduced can be extended to multilayered elastic systems of plain or cylindrical geometries. The underlying SCM technique is also general and can be extended to more complicated geometries and guiding structures and also to more general media, i.e., anisotropic or viscoelastic guides, and thereby, together with the leaky wave SCM, provides a methodology for all wave systems of this generic type, including those in electromagnetism.

ACKNOWLEDGMENTS

E.G. and R.V.C. are supported by the European Union H2020 FET Open "Boheme" Grant No. 863179.

[1]H. Lamb, "On waves in an elastic plate," Proc. R. Soc. A **81**, 114–128 (1916).
[2]D. N. Alleyne and P. Cawley, "Optimization of Lamb wave inspection techniques," NDT&E Int. **25**(1), 11–22 (1992).
[3]D. N. Alleyne, B. Pavlakovic, M. J. Lowe, and P. Cawley, "Rapid long-range inspection of chemical plant pipework using guided waves," Insight **557**, 180–196 (2001).
[4]P. Fromme, P. Wilcox, M. Lowe, and P. Cawley, "On the development and testing of a guided ultrasonic wave array for structural integrity monitoring," IEEE Trans. Ultrason. Ferroelectr. Freq. Control **53**(4), 777–785 (2006).
[5]R. Long, M. J. S. Lowe, and P. Cawley, "Attenuation characteristics of the fundamental modes that propagate in buried iron water pipes," Ultrasonics **41**(7), 509–519 (2003).
[6]P. D. Wilcox, M. J. S. Lowe, and P. Cawley, "Mode and transducer selection for long range lamb wave inspection," J. Intell. Mater. Syst. Struct. **12**(8), 553–565 (2001).
[7]F. Treyssède, K. L. Nguyen, A. S. Bonnet-BenDhia, and C. Hazard, "Finite element computation of trapped and leaky elastic waves in open stratified waveguides," Wave Motion **51**(7), 1093–1107 (2014).
[8]J. G. Scholte, "The range of existence of Rayleigh and Stoneley waves," Geophys. J. Int. **5**, 120–126 (1947).
[9]D. E. Chimenti and A. H. Nayfeh, "Leaky Lamb waves in fibrous composite laminates," J. Appl. Phys. **58**(12), 4531–4538 (1985).
[10]P. B. Nagy, W. R. Rose, and L. Adler, "A single transducer broadband technique for leaky Lamb wave detection," in *Review of Progress in Quantitative Nondestructive Evaluation* (Springer, Boston, MA, 1987), Vol. 6A, pp. 483–490.
[11]A. H. Nayfeh and D. E. Chimenti, "Propagation of guided waves in fluid-coupled plates of fiber-reinforced composite," J. Acoust. Soc. Am. **83**(5), 1736–1743 (1988).
[12]A. Snyder and J. Love, *Optical Waveguide Theory* (Chapman and Hall, London, 1983).
[13]J. Hu and C. R. Menyuk, "Understanding leaky modes: Slab waveguide revisited," Adv. Opt. Photonics **1**, 58–106 (2009).
[14]A. G. Every and G. A. D. Briggs, "Surface response of a fluid-loaded solid to impulsive line and point forces: Application to scanning acoustic microscopy," Phys. Rev. B **58**(3), 1601–1612 (1998).
[15]O. Lefeuvre, P. Zinin, and G. A. D. Briggs, "Leaky surface waves propagating on a fast on slow system and the implications for material characterization," Ultrasonics **36**, 229–232 (1998).
[16]F. B. Cegla, P. Cawley, and M. J. Lowe, "Fluid bulk velocity and attenuation measurements in non-Newtonian liquids using a dipstick sensor," Meas. Sci. Technol. **17**(2), 264–274 (2006).
[17]A. D. Stuart, "Acoustic radiation from submerged plates. I. Influence of leaky wave poles," J. Acoust. Soc. Am. **59**(5), 1160–1169 (1976).
[18]A. H. Nayfeh and P. B. Nagy, "Excess attenuation of leaky Lamb waves due to viscous fluid loading," J. Acoust. Soc. Am. **101**, 2649–2658 (1997).
[19]D. A. Kiefer, M. Ponschab, S. J. Rupitsch, and M. Mayle, "Calculating the full leaky Lamb wave spectrum with exact fluid interaction," J. Acoust. Soc. Am. **145**(6), 3341–3350 (2019).
[20]W. T. Thomson, "Transmission of elastic waves through a stratified solid medium," J. Appl. Phys. **21**(2), 89–93 (1950).
[21]N. A. Haskell, "The dispersion of surface waves on multilayered media," Bull. Seismol. Soc. Am. **54**(1), 431–438 (1964).
[22]L. Knopoff, "A matrix method for elastic wave problems," Bull. Seismol. Soc. Am. **54**(1), 431–438 (1964).
[23]B. Pavlakovic, M. J. S. Lowe, O. Alleyne, and P. Cawley, "Disperse: A general purpose program for creating dispersion curves," in *Review of Progress in Quantitative Nondestructive Evaluation* (Springer, Boston, MA, 1997), Vol. 16, pp. 185–192.
[24]M. J. S. Lowe, "Matrix techniques for modeling ultrasonic waves in multilayered media," IEEE Trans. Ultrason. Ferroelectr. Freq. Control **42**(4), 525–542 (1995).
[25]J. W. Dunkin, "Computation of modal solutions in layered, elastic media at high frequencies," Bull. Seismol. Soc. Am. **55**(2), 335–358 (1965).
[26]L. Gavrić, "Computation of propagative waves in free rail using a finite element technique," J. Sound Vib. **185**(3), 531–543 (1995).
[27]I. Bartoli, A. Marzani, F. Lanza di Scalea, and E. Viola, "Modeling wave propagation in damped waveguides of arbitrary cross-section," J. Sound Vib. **295**(3), 685–707 (2006).
[28]A. Marzani, E. Viola, I. Bartoli, F. Lanza di Scalea, and P. Rizzo, "A semi-analytical finite element formulation for modeling stress wave propagation in axisymmetric damped waveguides," J. Sound Vib. **318**(3), 488–505 (2008).
[29]M. Castaings and M. Lowe, "Finite element model for waves guided along solid systems of arbitrary section coupled to infinite solid media," J. Acoust. Soc. Am. **123**(2), 696–708 (2008).
[30]T. Hayashi and D. Inoue, "Calculation of leaky Lamb waves with a semi-analytical finite element method," Ultrasonics **54**(6), 1460–1469 (2014).
[31]A. T. I. Adamou and R. V. Craster, "Spectral methods for modelling guided waves in elastic media," J. Acoust. Soc. Am. **116**(3), 1524–1535 (2004).
[32]J. A. C. Weideman and S. C. Reddy, "A MATLAB differentiation matrix suite," ACM Trans. Math. Softw. **26**(4), 465–519 (2000).
[33]L. N. Trefethen, *Spectral Methods in Matlab* (SIAM, Philadelphia, 2008).
[34]J. P. Boyd, *Chebyshev and Fourier Spectral Methods*, 2nd ed. (Dover, Mineola, NY, 2000).
[35]F. Karpfinger, B. Gurevich, and A. Bakulin, "Modeling of wave dispersion along cylindrical structures using the spectral method," J. Acoust. Soc. Am. **124**(2), 859–865 (2008).
[36]T. Zharnikov, D. Syresin, and C. J. Hsu, "Application of the spectral method for computation of the spectrum of anisotropic waveguides," Proc. Mtgs. Acoust. **19**, 045065 (2013).
[37]F. H. Quintanilla, Z. Fan, M. J. S. Lowe, and R. V. Craster, "Guided waves' dispersion curves in anisotropic viscoelastic single- and multi-layered media," Proc. R. Soc. A **471**(2183), 20150268 (2015).
[38]F. H. Quintanilla, M. J. S. Lowe, and R. V. Craster, "Modeling guided elastic waves in generally anisotropic media using a spectral collocation method," J. Acoust. Soc. Am. **137**(3), 1180–1194 (2015).
[39]F. H. Quintanilla, M. J. S. Lowe, and R. V. Craster, "Full 3D dispersion curve solutions for guided waves in generally anisotropic media," J. Sound Vib. **363**, 545–559 (2016).
[40]A. Grabowska, "Propagation of elastic wave in solid layer-liquid system," Arch. Acoust. **4**(1), 57–63 (1979), available at https://acoustics.ippt.pan.pl/index.php/aa/article/view/3356.
[41]S. I. Rokhlin, D. E. Chimenti, and A. H. Nayfeh, "On the topology of the complex wave spectrum in a fluid-coupled elastic layer," J. Acoust. Soc. Am. **85**(3), 1074–1080 (1989).

05 July 2024 14:23:42

https://doi.org/10.1121/10.0013897

[42]M. Mazzotti, I. Bartoli, and A. Marzani, "Ultrasonic leaky guided waves in fluid-coupled generic waveguides: Hybrid finite-boundary element dispersion analysis and experimental validation," J. Appl. Phys. **115**(14), 143512 (2014).
[43]A. Hood, "Localizing the eigenvalues of matrix-valued functions: Analysis and applications," Ph.D. thesis, Cornell University, Ithaca, NY, 2017.
[44]D. S. Mackey, N. Mackey, C. Mehl, and V. Mehrmann, "Structured polynomial eigenvalue problems: Good vibrations from good linearizations," SIAM J. Matrix Anal. Appl. **28**(4), 1029–1051 (2006).
[45]Z. Fan, M. J. S. Lowe, M. Castaings, and C. Bacon, "Torsional waves propagation along a waveguide of arbitrary cross section immersed in a perfect fluid," J. Acoust. Soc. Am. **124**(4), 2002–2010 (2008).
[46]F. H. Quintanilla, "Pseudospectral collocation method for viscoelastic guided wave problems in generally anisotropic media," Ph.D. thesis, Imperial College London, London, 2016.
[47]F. H. Quintanilla, M. J. S. Lowe, and R. V. Craster, "The symmetry and coupling properties of solutions in general anisotropic multilayer waveguides," J. Acoust. Soc. Am. **141**(1), 406–418 (2017).
[48]J. D. Achenbach, *Wave Propagation in Elastic Solids* (North-Holland, Amsterdam, 1973), p. 425.
[49]J. L. Rose, *Ultrasonic Guided Waves in Solid Media* (Cambridge University, New York, 2014).
[50]See supplementary material at https://www.scitation.org/doi/suppl/10.1121/10.0013897 for the derivation of the momentum and interface equations, a brief discussion on the theory of differentiation matrices, and a discussion on the choice of the complex parameters ζ_{fj}.
[51]N. F. Declercq, R. Briers, J. Degrieck, and O. Leroy, "The history and properties of ultrasonic inhomogeneous waves," IEEE Trans. Ultrason. Ferroelectr. Freq. Control **52**(5), 776–791 (2005).
[52]B. Fornberg, *A Practical Guide to Pseudospectral Methods* (Cambridge University, Cambridge, UK, 1996).
[53]A. Abdrabou, A. M. Heikal, and S. S. A. Obayya, "Efficient rational Chebyshev pseudo-spectral method with domain decomposition for optical waveguides modal analysis," J. Opt. Soc. Am. **24**(10), 10495–10511 (2016).
[54]M. J. S. Lowe and B. Pavlakovic, *Disperse: A System for Generating Dispersion Curves: User's Manual* (Imperial College London, London, 2013).
[55]O. Diligent, M. J. S. Lowe, E. Le Clézio, M. Castaings, and B. Hosten, "Prediction and measurement of nonpropagating Lamb modes at the free end of a plate when the fundamental antisymmetric mode A_0 is incident," J. Acoust. Soc. Am. **113**(6), 3032–3042 (2003).
[56]T. K. Vogt, M. J. S. Lowe, and P. Cawley, "Measurement of the material properties of viscous liquids using ultrasonic guided waves," IEEE Trans. Ultrason. Ferroelectr. Freq. Control **51**(6), 737–747 (2004).
[57]F. B. Cegla, P. Cawley, and M. J. S. Lowe, "Material property measurement using the quasi-Scholte mode—A waveguide sensor," J. Acoust. Soc. Am. **117**(3), 1098–1107 (2005).
[58]J. Ma, M. J. Lowe, and F. Simonetti, "Feasibility study of sludge and blockage detection inside pipes using guided torsional waves," Meas. Sci. Technol. **18**(8), 2629–2641 (2007).
[59]E. Leinov, M. J. S. Lowe, and P. Cawley, "Ultrasonic isolation of buried pipes," J. Sound Vib. **363**, 225–239 (2016).

05 July 2024 14:23:42